

Dilute spin glass at zero temperature in general dimension

Lior Klein

School of Physics and Astronomy, Beverly and Raymond Sackler Faculty of Exact Sciences, Tel Aviv University, 69978 Tel Aviv, Israel

Joan Adler

School of Physics and Astronomy, Beverly and Raymond Sackler Faculty of Exact Sciences, Tel Aviv University, 69978 Tel Aviv, Israel
and Department of Physics, Technion-Israel Institute of Technology, 32000 Haifa, Israel

Amnon Aharony

School of Physics and Astronomy, Beverly and Raymond Sackler Faculty of Exact Sciences, Tel Aviv University, 69978 Tel Aviv, Israel

A. B. Harris

School of Physics and Astronomy, Beverly and Raymond Sackler Faculty of Exact Sciences, Tel Aviv University, 69978 Tel Aviv, Israel
and Department of Physics, University of Pennsylvania, Philadelphia, Pennsylvania 19104

Yigal Meir

School of Physics and Astronomy, Beverly and Raymond Sackler Faculty of Exact Sciences, Tel Aviv University, 69978 Tel Aviv, Israel

(Received 6 March 1989)

We study the zero-temperature critical behavior of the dilute Ising spin glass. In our model nearest-neighbor exchange interactions randomly assume the values $+J$, 0 , $-J$ with probabilities $p/2$, $1-p$, and $p/2$, respectively. We have generated 15th-order series for the Edwards-Anderson spin-glass susceptibility as a function of concentration p on hypercubic lattices in general dimension. Their analysis leads to critical concentrations and exponents that differ from those of percolation.

I. INTRODUCTION

Elucidation of the properties of the diluted Ising spin glass (DSG) has been the focus of considerable recent interest.¹⁻⁹ The Hamiltonian of this system is written

$$\mathcal{H} = - \sum_{\langle i,j \rangle} J_{ij} S_i S_j, \quad (1.1)$$

where $S_i = \pm 1$, while the nearest-neighbor exchange variables $J_{ij} = J_{ji}$ assume the quenched values $-J$, 0 , and J with the respective probabilities p_2 , $1-p_1-p_2$, and p_1 . When $p_2 = 0$, this problem reduces to that of the dilute Ising ferromagnet, and the transition temperature $T_c(p_1)$ decreases monotonically from its pure Ising value $T_c(1)$ to zero at the percolation threshold, $p_1 = p_c$. The transition at $T=0$, as a function of p_1 , is characterized by the percolation critical behavior.

Much of the recent interest in this problem concerned the three-dimensional phase diagram, in the $T-p_1-p_2$ space.^{1,5} For fixed p_1 and p_2 , one qualitatively expects a transition from the paramagnetic state into an ordered magnetic state (ferromagnetic, antiferromagnetic, or spin glass), at a temperature which decreases with (p_1+p_2) . In this paper we concentrate on the symmetric case, $p_1 = p_2 = p/2$. Here, one expects spin-glass (SG) ordering

below $T_g(p)$, with $T_g(p)$ decreasing to zero at p_{SG} . We shall specifically address two questions: First, is p_{SG} equal to the percolation threshold p_c , as recently suggested,⁶ or is it higher than p_c , as indicated in Refs. 4, 5, and 7-9? Second, what is the critical behavior of the zero-temperature dilute spin glass (ZTDSG), i.e., the symmetric problem at $T=0$ with p approaching p_{SG} ?

A convenient method to approach the second problem follows the treatment of Stephen and Grest¹⁰ of the percolation problem. They used the "replica trick," in which the quenched averaged free energy is calculated via

$$F = -[\ln Z]_c = -\lim_{n \rightarrow 0} [Z^n - 1]_c / n, \quad (1.2)$$

where $[]_c$ denotes the configurational average over the J_{ij} 's. In this method, each site is assigned n spin variables $\{S_i^\alpha, \alpha = 1, 2, \dots, n\}$, having 2^n states. The average replicated Hamiltonian then involves $(2^n - 1)$ order parameters, $S_i^\alpha, \mu_i^{\alpha\beta} \equiv S_i^\alpha S_i^\beta, \dots, \mu_i^{\alpha\beta \dots w} \equiv S_i^\alpha S_i^\beta \dots S_i^w, \dots, \mu_i^{1 \dots n} \equiv S_i^1 \dots S_i^n$, and one can study the critical properties via the generalized susceptibilities

$$\chi^{(q)} \equiv \sum_j [\langle S_i S_j \rangle^q]_c \equiv \sum_j \langle \mu_i^{\alpha_1 \dots \alpha_q} \mu_j^{\alpha_1 \dots \alpha_q} \rangle_n. \quad (1.3)$$

Here $\langle \rangle$ denotes the thermal average for a given quenched configuration, while $\langle \rangle_n$ denotes the average using the replicated (nonrandom) Hamiltonian.

For the percolation problem ($T=0$, $p_2=0$), all the 2^n states are equivalent. This implies that all the $\chi^{(q)}$'s diverge at p_c as $|p-p_c|^{-\gamma_p}$, with the exponent γ_p resulting from the limit $q \rightarrow 1$ ($n \rightarrow 0$) of the $q=2^n$ -state Potts model.¹⁰

For the ZTDSG problem, $\chi^{(q)}$ vanishes for odd q , and one is left with 2^{n-1} states (and order parameters). Taking the limit $T \rightarrow 0$ before $n \rightarrow 0$, Aharony¹ and Giri and Stephen² found that all these states are equivalent, yielding the critical behavior of the $q \rightarrow \frac{1}{2}$ limit of the q -state Potts models. However, it was soon realized that this order of limits is inappropriate, since it eliminates some of the frustration effects.³ More recently, Harris⁴ used the limit of large coordination number ($z = \sigma + 1 \gg 1$), which means a relatively small number of loops, or high dimensionality, to show that the $\chi^{(2q)}$'s diverge at *different* thresholds, $p_c < p_2 < p_4 < \dots$. At the ZTDSG transition, we expect the Edwards-Anderson susceptibility $\chi_{EA} \equiv \chi^{(2)}$ to diverge. If Harris's result persists at low dimensionalities, this implies that the divergence of χ_{EA} at p_{SG} is governed only by the SG order parameters $\mu_i^{\alpha\beta}$, similar to the spin-glass thermal transition at $p=1$. One would thus expect the same critical behavior along the whole line $T_g(p)$. On the other hand, if the thresholds p_{2q} are very close to each other, then the crossover at $T=0$ from percolation to the $\frac{1}{2}$ state Potts and/or to the thermal behavior may be slow and complicated. Indeed, preliminary series expansions of χ_{EA} by Aharony and Binder (AB),⁵ based on eight terms in p , were unable to separate $p_{SG}=p_2$ from p_c , and the exponents were close to those of percolation. In this paper we extend these series by seven additional terms in order to obtain improved accuracy.

In order to evaluate the significance of our new results we shall need to compare them with the best available estimates for the three systems: percolation, the $q \rightarrow \frac{1}{2}$ limit of the q -state Potts model, and the thermal spin glass, in general dimension. A summary of the best extant ex-

ponent estimates for the susceptibility exponent γ for percolation and spin-glass models in general dimension is given in Table I. For percolation, the third-order ϵ expansion¹¹ converges very well, and our new 15th-order series results¹² are in excellent agreement with its predictions for $d=4,5$. In three dimensions (3D) the new series and recent simulation¹³ results for both thresholds and exponents are in excellent agreement. There are exact¹⁴ results for 2D percolation and the 2D $q = \frac{1}{2}$ Potts model ($\gamma=3.267$). For the higher-dimensional $q = \frac{1}{2}$ Potts model and the thermal spin glass, we will have a serious problem with comparisons. For the thermal spin glass the third-order ϵ expansion¹⁵ fails to converge, and the series results are also problematic in the lower dimensions. We shall discuss this in more detail in the conclusion and in Ref. 16. Previous exponent estimates for the thermal spin glass are given in Refs. 17 and 18. For the $q = \frac{1}{2}$ state Potts model the best general result is of first order in ϵ , videlicet $\gamma=1+3\epsilon/17$. If we compare the first-order results for percolation ($\gamma=1+\epsilon/7$), and thermal spin glass ($\gamma=1+\epsilon$), with the more accurate calculations we see that the first-order results are not very reliable. Thus from a practical viewpoint we do not have any $\frac{1}{2}$ state Potts results available for comparison in general dimension; and it is really only for percolation that we have a complete picture.

The remainder of this paper is organized as follows. In Sec. II we describe the series generation, and present the series in Table II. The analysis is discussed in Sec. III, with results for the thresholds from both the present and previous calculations being given in Table III. Table IV contains the results of our exponent measurements. We conclude in Sec. IV with a discussion.

II. GENERATION OF THE SERIES

In order to determine the location and nature of the zero-temperature dilute spin-glass (ZTDSG) critical point we have obtained low-concentration 15th-order exact power series expansions of the Edwards-Anderson susceptibility,

TABLE I. Estimates for γ from the literature.

d	2	3	4	5
Thermal spin glass				
Series ^a	5.3±0.3	2.9±0.5	2.0±0.4	
Series ^b				2.23
Series ^c			2.0±0.2	1.7±0.2
Percolation				
Exact ^d	2.38			
Series ^e		1.805±0.02	1.435±0.015	1.185±0.005
ZTDSG				
Series ^f	2.7	2.0	1.4	

^aReference 27.

^bReference 18.

^cReference 16.

^dReference 14.

^eReference 12.

^fReference 5.

$$\begin{aligned}\chi^{\text{EA}} &= \frac{1}{N} \sum_{i,j} [\langle S_i S_j \rangle^2]_{\text{av}} = 1 + \sum_{mn} a(m,n) p^m d^n \\ &= 1 + \sum_m b(m) p^m \sim (p_{\text{SG}} - p)^{-\gamma}\end{aligned}\quad (2.1)$$

for the bond dilute $\pm J$ Ising model on general d -dimensional hypercubic lattices. This calculation is part of a project to calculate extended series for many systems in general dimension; recent calculations include lattice animals,¹⁹ isotropic random percolation,¹² and the finite-temperature dilute and nondilute Ising spin-glass system.¹⁶ The identification of and distinction between different critical behaviors and thresholds for the ZTDSG required citation of some of the new results for percolation and spin glasses in Table I.

The series have been generated via the Harris²⁰ scheme that uses only no-free-end (NFE) diagrams. This increases the efficiency of the calculation considerably relative to using total enumerations of the graphs as was done by AB. A detailed description of the application of this method to the calculation of the first three moments of the $\pm J$ spin glass will be given in Ref. 16, so we give below only a brief survey. According to the Harris scheme we write

$$\chi^{\text{EA}} = \chi_{\text{CT}}^{\text{EA}} + \sum_{\Gamma} W_d(\Gamma) \delta\chi(\Gamma)_c, \quad (2.2)$$

where

$$\chi_{\text{CT}}^{\text{EA}} = (1+p)/(1-\sigma p)$$

and $\sigma = 2d - 1$. $\chi_{\text{CT}}^{\text{EA}}$ is the susceptibility for the Cayley tree that has the same coordination number ($2d$) as the

d -dimensional hypercubic lattice. $W_d(\Gamma)$ is the weight of the NFE diagram Γ , and $\delta\chi(\Gamma)_c$ is the cumulant contribution of this diagram to χ^{EA} .

We calculate $\delta\chi$ for each of the NFE diagrams, which are tabulated through to 15th order,²¹ by introducing a function $g(\mathbf{S}_i, h)$ into the replicated partition function

$$[Z^n]_c = \text{Tr} \prod_i \rho_i \prod_{\langle i,j \rangle} f_{ij},$$

where

$$f_{ij} = \left[\exp \left[\beta J_{ij} \sum_{\alpha} S_i^{\alpha} S_j^{\alpha} \right] \right]_c$$

and

$$\rho_i = \exp \left[h \sum_{\alpha < \beta} S_i^{\alpha} S_i^{\beta} \right].$$

We write

$$[Z^n]_c = \text{Tr} \left[\prod_i \rho_i g(\mathbf{S}_i, h)^z \prod_{\langle i,j \rangle} \frac{f_{ij}}{g(\mathbf{S}_i, h)g(\mathbf{S}_j, h)} \right], \quad (2.3)$$

where $z = 2d$, and $\mathbf{S}_i = \{S_i^{\alpha}\}$, with $\alpha = 1, \dots, n$ being the replica index and n the replica number. To eliminate free-end diagrams, $g(\mathbf{S}_i, h)$ should obey²⁰

$$g(\mathbf{S}_i, h) = \frac{\text{Tr}_{\mathbf{S}_j} g(\mathbf{S}_j, h)^{\sigma} \rho_j f_{ij}}{\text{Tr}_{\mathbf{S}_j} g(\mathbf{S}_j, h)^z \rho_j}. \quad (2.4)$$

After solving Eq. (2.4) we substitute $g(\mathbf{S}_i, h)$ into (2.3), and by differentiating (2.3) twice by the field h and taking the limits $n \rightarrow 0$ and $h \rightarrow 0$, we finally obtain the contribution of the diagram Γ to the zero-temperature spin-glass susceptibility,

$$\delta\chi(\Gamma) = \frac{1}{(1-\sigma p)^2} \left[\sum_i z_i^2 p^2 - 2n_b(\Gamma) p(1+p) + \sum_{k \neq l} \{1 + [1 - z_k(\Gamma)]p\} \{1 + [1 - z_l(\Gamma)]p\} \sum_{\Gamma' \in \Gamma} P(\Gamma', p) C_{kl}(\Gamma') \right], \quad (2.5)$$

where $z_i(\Gamma)$ is the number of neighbors of site i in the diagram Γ , and $n_b(\Gamma)$ the total number of bonds in diagram Γ . Γ' is a subdiagram of Γ , and the probability of obtaining a subdiagram Γ' when we average over the dilution is

$$P(\Gamma', p) = p^{n_b(\Gamma')} (1-p)^{n_b(\Gamma) - n_b(\Gamma')},$$

where $n_b(\Gamma')$ is the number of bonds in subdiagram Γ' . C_{kl} is the Edwards-Anderson correlation between the two sites k, l , and equals $[\langle S_k S_l \rangle^2]_c$. The early terms of the new series are in agreement with AB modulo some very minor discrepancies that are caused by misprints in AB. We are certain that the NFE graph enumerations are reliable for both spin-glass and percolation problems (and thence for the ZTDSG), as the 15th-order series that we

generate^{12,16} from them agree with existing series^{17,22} for both problems in low dimensions. The coefficients $a(m, n)$ from Eq. (2.1) of the series are given in Table II.

The series are extremely well behaved, with the coefficients $b(m)$ being positive in all integer dimensions, and monotonically increasing for $d \geq 3$. To illustrate this we quote the $b(m)$ to three-digit accuracy in 3D. The terms for $m = 1, \dots, 15$ are 6, 30, 150, 675, 3.13×10^3 , 1.32×10^4 , 5.83×10^4 , 2.3×10^5 , 1.03×10^6 , 4.05×10^6 , 1.75×10^7 , 6.70×10^7 , 2.90×10^8 , 1.08×10^9 , and 4.73×10^9 . As one can see, the ratio between successive terms does not fluctuate very much. In contrast, the thermal spin-glass series for χ^{EA} have alternating signs in 3D. More accurate values of the coefficients can be calculated from the data in Table II.

TABLE II. Series coefficients for χ^{EA} , where $\chi^{\text{EA}} = 1 + \sum_{mn} a(m,n)p^m d^n$.

M	N	$a(m,n)$	M	N	$a(m,n)$
1	1	0.000 000 000 000 000	2	1	0.000 000 000 000 000
2	2	0.000 000 000 000 000	3	1	0.000 000 000 000 000
3	2	0.000 000 000 000 000	3	3	0.000 000 000 000 000
4	1	-0.125 000 000 000 000 $\times 10^2$	4	2	0.125 000 000 000 000 $\times 10^2$
4	3	0.000 000 000 000 000	4	4	0.000 000 000 000 000
5	1	-0.210 000 000 000 000 $\times 10^2$	5	2	0.210 000 000 000 000 $\times 10^2$
5	3	0.000 000 000 000 000	5	4	0.000 000 000 000 000
5	5	0.000 000 000 000 000	6	1	-0.224 055 555 555 555 $\times 10^3$
6	2	0.367 166 666 666 666 $\times 10^3$	6	3	-0.143 111 111 111 111 $\times 10^3$
6	4	0.000 000 000 000 000	6	5	0.000 000 000 000 000
6	6	0.000 000 000 000 000	7	1	0.886 944 444 444 444 $\times 10^3$
7	2	-0.145 705 555 555 555 $\times 10^4$	7	3	0.570 111 111 111 111 $\times 10^3$
7	4	0.000 000 000 000 000	7	5	0.000 000 000 000 000
7	6	0.000 000 000 000 000	7	7	0.000 000 000 000 000
8	1	0.989 059 722 222 222 $\times 10^4$	8	2	-0.192 669 583 333 333 $\times 10^5$
8	3	0.117 311 111 111 111 $\times 10^5$	8	4	-0.235 475 000 000 000 $\times 10^4$
8	5	0.000 000 000 000 000	8	6	0.000 000 000 000 000
8	7	0.000 000 000 000 000	8	8	0.000 000 000 000 000
9	1	-0.467 875 388 888 888 $\times 10^5$	9	2	0.936 192 722 222 222 $\times 10^5$
9	3	-0.585 261 333 333 333 $\times 10^5$	9	4	0.113 819 000 000 000 $\times 10^5$
9	5	0.312 500 000 000 000 $\times 10^3$	9	6	0.000 000 000 000 000
9	7	0.000 000 000 000 000	9	8	0.000 000 000 000 000
9	9	0.000 000 000 000 000	10	1	-0.719 566 346 944 444 $\times 10^6$
10	2	0.160 726 554 194 444 $\times 10^7$	10	3	-0.125 950 463 944 444 $\times 10^7$
10	4	0.427 582 566 666 666 $\times 10^6$	10	5	-0.564 021 222 222 222 $\times 10^5$
10	6	0.625 000 000 000 000 $\times 10^3$	10	7	0.000 000 000 000 000
10	8	0.000 000 000 000 000	10	9	0.000 000 000 000 000
10	10	0.000 000 000 000 000	11	1	0.311 073 803 265 872 $\times 10^7$
11	2	-0.729 493 746 496 030 $\times 10^7$	11	3	0.607 017 394 928 571 $\times 10^7$
11	4	-0.216 626 836 460 317 $\times 10^7$	11	5	0.278 988 292 063 491 $\times 10^6$
11	6	0.555 555 555 555 556 $\times 10^2$	11	7	0.125 000 000 000 000 $\times 10^4$
11	8	0.000 000 000 000 000	11	9	0.000 000 000 000 000
11	10	0.000 000 000 000 000	11	11	0.000 000 000 000 000
12	1	0.729 656 404 493 169 $\times 10^8$	12	2	-0.180 782 346 645 061 $\times 10^9$
12	3	0.167 777 029 477 126 $\times 10^9$	12	4	-0.751 324 955 813 112 $\times 10^8$
12	5	0.166 997 203 014 726 $\times 10^8$	12	6	-0.152 890 911 265 432 $\times 10^7$
12	7	-0.113 888 888 888 889 $\times 10^4$	12	8	0.250 000 000 000 000 $\times 10^4$
12	9	0.000 000 000 000 000	12	10	0.000 000 000 000 000
12	11	0.000 000 000 000 000	12	12	0.000 000 000 000 000
13	1	-0.254 103 676 069 280 $\times 10^9$	13	2	0.678 364 192 531 764 $\times 10^9$
13	3	-0.690 282 099 418 361 $\times 10^9$	13	4	0.340 262 523 719 297 $\times 10^9$
13	5	-0.819 453 285 667 176 $\times 10^8$	13	6	0.769 074 227 860 671 $\times 10^7$
13	7	0.134 233 024 691 357 $\times 10^5$	13	8	-0.477 777 777 777 778 $\times 10^4$
13	9	0.500 000 000 000 000 $\times 10^4$	13	10	0.000 000 000 000 000
13	11	0.000 000 000 000 000	13	12	0.000 000 000 000 000
13	13	0.000 000 000 000 000	14	1	-0.953 043 555 667 327 $\times 10^{10}$
14	2	0.257 097 092 989 665 $\times 10^{11}$	14	3	-0.271 368 449 001 112 $\times 10^{11}$
14	4	0.146 994 632 570 225 $\times 10^{11}$	14	5	-0.439 576 632 715 557 $\times 10^{10}$
14	6	0.701 763 332 276 203 $\times 10^9$	14	7	-0.479 083 606 525 573 $\times 10^8$
14	8	0.238 118 827 160 494 $\times 10^5$	14	9	-0.145 555 555 555 555 $\times 10^5$
14	10	0.100 000 000 000 000 $\times 10^5$	14	11	0.000 000 000 000 000
14	12	0.000 000 000 000 000	14	13	0.000 000 000 000 000
14	14	0.000 000 000 000 000	15	1	0.262 407 900 926 066 $\times 10^{11}$
15	2	-0.775 694 318 509 213 $\times 10^{11}$	15	3	0.914 204 795 517 114 $\times 10^{11}$
15	4	-0.557 493 969 500 021 $\times 10^{11}$	15	5	0.187 162 694 985 778 $\times 10^{11}$
15	6	-0.329 627 612 241 148 $\times 10^{10}$	15	7	0.237 261 553 155 515 $\times 10^9$
15	8	0.276 784 074 074 074 $\times 10^6$	15	9	0.465 543 209 876 543 $\times 10^5$
15	10	-0.391 111 111 111 111 $\times 10^5$	15	11	0.200 000 000 000 000 $\times 10^5$
15	12	0.000 000 000 000 000	15	13	0.000 000 000 000 000
15	14	0.000 000 000 000 000	15	15	0.000 000 000 000 000

TABLE III. Estimates for p_c .

d	Percolation Ref. 12	Percolation ($1/\sigma$) Ref. 26	DSG (15th) This work	DSG (AB) Ref. 5	DSG ($1/\sigma$) Ref. 4	DSG (PB) Ref. 6
2	$\frac{1}{2}$ (Exact)	0.518 5	0.69 ± 0.02	0.55	0.566 5	
3	0.2488 ± 0.0002	0.232 0	$0.266 5 \pm 0.001 0$	0.26	0.240 2	$0.22 - 0.25$
4	$0.160 05 \pm 0.000 15$	0.153 3	$0.164 5 \pm 0.000 5$	0.16	0.155 9	$0.155 - 0.166$
5	$0.118 19 \pm 0.000 04$	0.115 7	$0.120 1 \pm 0.000 5$		0.116 8	$0.117 - 0.120$
6	$0.094 20 \pm 0.000 1$	0.093 30	$0.095 08 \pm 0.000 05$		0.093 91	$0.0935 - 0.0955$
7	$0.078 685 \pm 0.000 03$	0.078 32	$0.079 15 \pm 0.000 02$		0.078 68	$0.078 - 0.0795$
8	$0.067 70 \pm 0.000 05$	0.067 56	$0.067 98 \pm 0.000 05$	0.068	0.067 78	$0.0673 - 0.0683$
9	$0.059 500 \pm 0.000 05$	0.059 42	$0.059 67 \pm 0.000 05$		0.059 57	

III. ANALYSIS

The methods used in the analysis of the series have been discussed in depth in Refs. 12 and 19. There and here, we have analyzed the series for integer dimensions $1 \leq d \leq 9$. We assume critical behavior that includes non-analytic confluent corrections to scaling, which arise from the irrelevant operators. This gives the form

$$\chi^{\text{EA}} \sim (p_{\text{SG}} - p)^{-\gamma} [1 + a(p_{\text{SG}} - p)^{\Delta_1}], \quad d \neq 6 \quad (3.1)$$

and

$$\chi^{\text{EA}} \sim (p_{\text{SG}} - p)^{-\gamma} |\ln|p_{\text{SG}} - p||^{\theta}, \quad d = 6. \quad (3.2)$$

We have obtained graphs of Padé approximants to γ as a function of the correction exponent Δ_1 for selected thresholds in the range $p > p_c$. All analyses were made by two different algorithms^{22,23} for fitting Eq. (3.1) which we call $M1$ and $M2$. We have fitted Eq. (3.2) with an analysis method from Ref. 24. In addition to these threshold-biased analyses, we have made estimates of γ via a technique²⁵ that is not threshold biased. This method¹² involves division of series term-by-term, mapping the threshold to 1.0. Since we only have one series in this case, we have divided the terms of the square of the series by the terms of the series itself.

In the threshold-biased analyses we searched for the threshold that gave optimal convergence of the different approximants. In each case we checked for consistency between the exponents at the best converged thresholds and the exponents obtained from the unbiased analyses. This consistency was achieved in all dimensions above two. It must be noted that convergence is very good for all the series above two dimensions.

We present the results of the analyses in Tables III (thresholds) and IV (exponents). The results of threshold

estimates for percolation from our new series¹² and from the $1/\sigma$ expansion for percolation²⁶ are given in Table III for comparison purposes. The errors for all our new results have been estimated as follows. For the results of the divided series in Table IV there is an error of about ± 0.5 of the last quoted digit from limit of reading problems. The errors for the threshold-biased exponents and the thresholds themselves are quoted explicitly in the tables on a case-by-case basis. These are based on the extremes of the regions of convergence of the Padé approximants for the range of threshold choices that were consistent with the divided values. We believe that it is very unlikely that the true result for a series of this length lies outside the ranges that we have given, but there may be effects that appear only in higher-order diagrams that we cannot take into account. We quote four significant figures for the $1/\sigma$ expansion. The expansion may not be accurate for so many figures, but errors are difficult to estimate in this expansion.

From a comparison of the results from the 15-term series for percolation from Ref. 12 and the results of the present calculation for the dilute spin glass, we see that there is no overlap of the ZTDSG threshold p_{SG} with the percolation critical point p_c . This distinction holds in all dimensions. We consider these results to be decisive, and note that in most cases the distinction would hold even if the error ranges for both sets of results were substantially increased. The high-dimensional thresholds are close to the $1/\sigma$ expansion values^{26,4} for both the percolation²⁶ and ZTDSG (Ref. 4) problems. The difference between percolation and ZTDSG values is about the same for each technique, although the $1/\sigma$ results are consistently lower. Overall, we obtain a clear separation between percolation and ZTDSG thresholds.

The exponent estimates are not as clearcut as the

TABLE IV. Our estimates for γ and Δ_1 for the ZTDSG.

d	Divided series ($\Delta_1 = 1.0$)		Divided series (best convergence)			Threshold biased		
	$\gamma(M1)$	$\gamma(M2)$	$\gamma(M1)$	$\Delta_1(M1)$	$\gamma(M2)$	$\Delta_1(M2)$	γ	Δ_1
2							$5.4^{+0.4}_{-0.8}$	1.7 ± 0.3
3		2.1	2.0	1.4	2.1	1.2	2.05 ± 0.05	1.2 ± 0.2
4	1.44	1.48	1.45	1.5	1.46	0.9	1.46 ± 0.06	$1.0^{+0.5}_{-0.3}$
5	1.2	1.22	1.2	1.0	1.22	0.7	1.22 ± 0.07	1.0 ± 0.7

threshold ones, and we shall discuss these on a dimension-by-dimension basis. It must again be emphasized that with the exception of percolation and the 2D $q = \frac{1}{2}$ Potts model, we do not have clear exponent

values for comparison purposes. In 2D we can observe from Tables I and III that our estimate of $5.4_{-0.8}^{+0.4}$ has definitely crossed over from the exact percolation ($\gamma = 2.38$) and $q = \frac{1}{2}$ Potts model ($\gamma = 3.267$) critical ex-

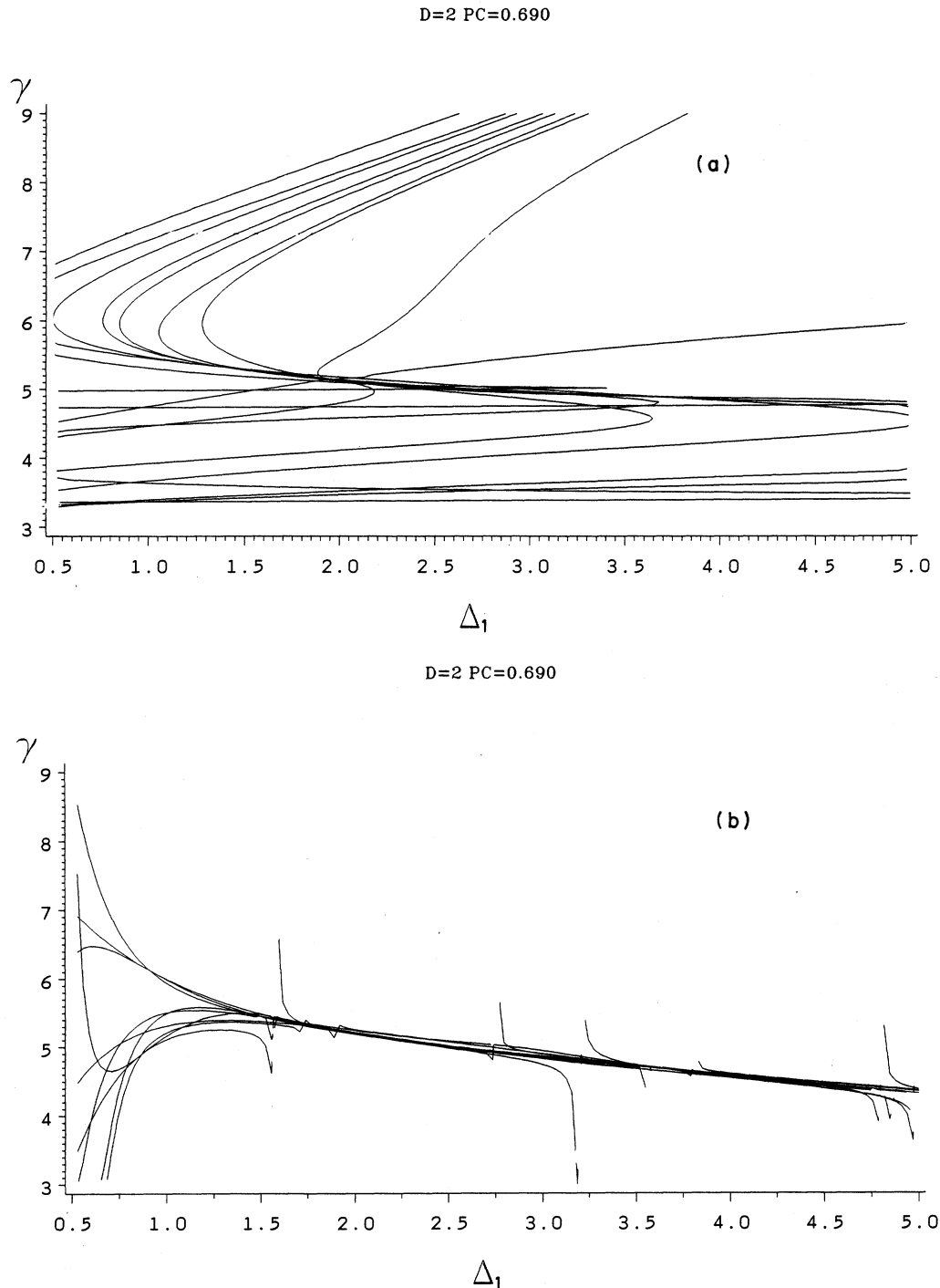


FIG. 1. Graphs of selected central and near diagonal Padé approximants to (a) γ as a function of Δ_1 from the $M1$ analysis at $p_c = 0.69$ at $d=2$; (b) γ as a function of Δ_1 from the $M2$ analysis at $p_c = 0.69$ at $d=2$; (c) $\gamma + 1$ as a function of Δ_1 from the $M2$ analysis of the divided series in $d=3$; (d) γ as a function of Δ_1 from the $M2$ analysis at $p_c = 0.16575$ at $d=4$; (e) $\gamma + 1$ as a function of Δ_1 from the $M2$ analysis of the divided series in $d=5$.

ponents. This is the first decisive observation that the two-dimensional ZTDSG is in neither universality class. It is rather tantalizing to suggest that our observed exponent corresponds to the zero-temperature¹⁷ spin-glass exponent of $\gamma = 5.3 \pm 0.3$. This estimate is based on the threshold-biased results alone as the divided series failed to converge. We note that use of $M2$ alone in this case

gives ambivalent results, there being convergence near $p = \frac{1}{2}$, then a degradation followed by an improvement in convergence as p is increased. However, $M1$ gives convergence in the region of 0.69 only, and thus our overall conclusion is that the correct p_{SG} is in this region. Graphs of Padé approximants to γ as a function of Δ_1 at $p = 0.69$ for $M1$ and $M2$ are given in Figs. 1(a) and 1(b).

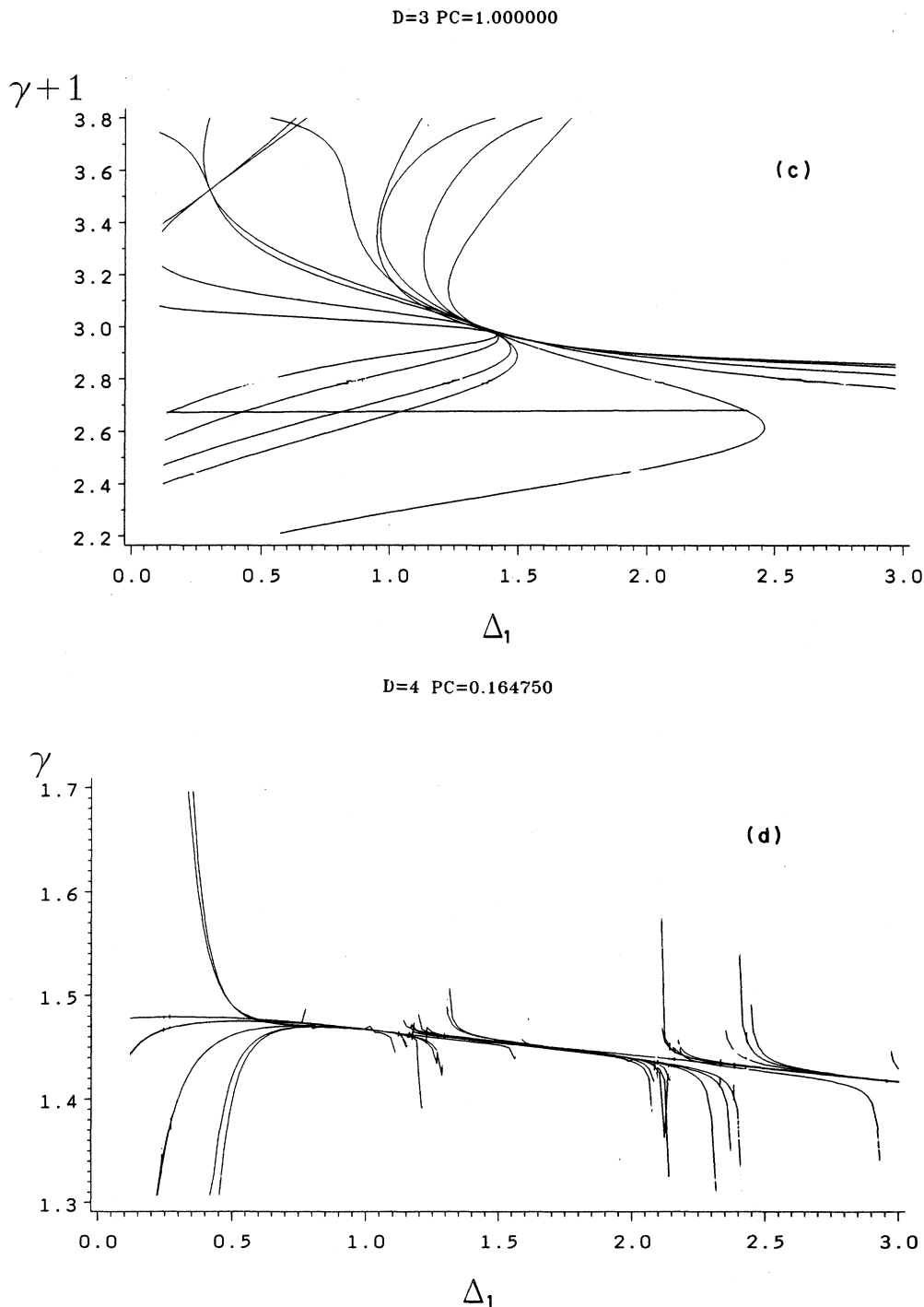


FIG. 1. (Continued).

D=5 PC=1.000000

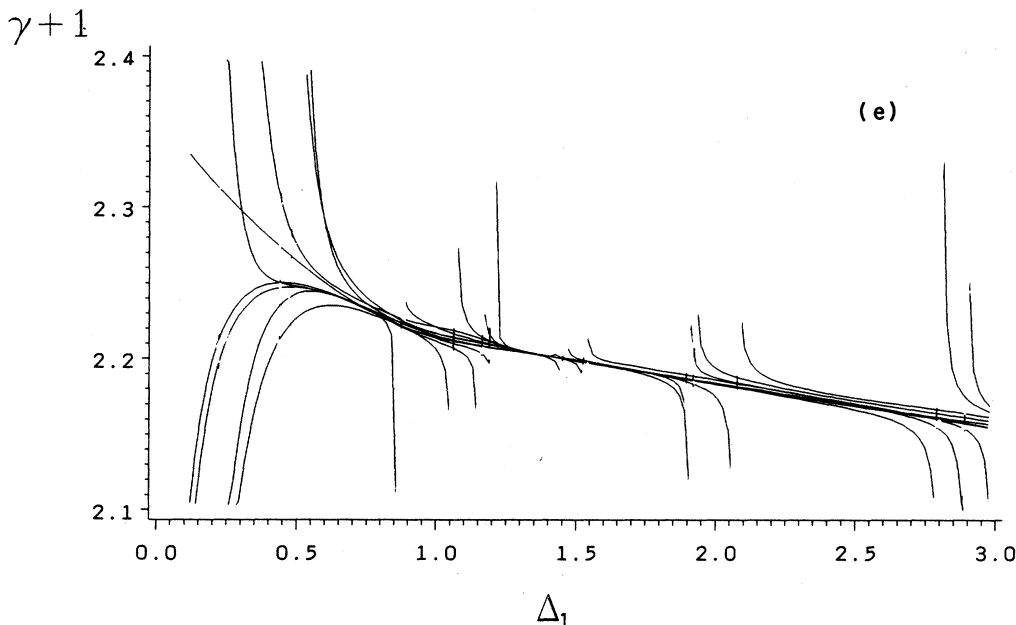


FIG. 1. (Continued).

The divided series analyses are poorly converged at $d=2$. By analogy with the thermal spin glass, which has order only at $T=0$, it could be implied that the threshold for the $d=2$ case should be at $p=1.0$. We cannot rule out this possibility from a 15-term series. We have, however, made a careful study of threshold as a function of series size and see that the convergence to 0.69 from $M1$ sets in by 12th order, and does not move as the series length is further increased.

In 3D we have made a comprehensive study of the exponent as a function of series length for the ZTDSG using the unbiased approach and find, for example, $\gamma=1.8$ at 11 terms from $M1$. For the 15-term series we find $\gamma=2.05\pm 0.05$, from the threshold-biased analysis, and consistent results from the divided series. A graph of the divided series with $M1$ is given in Fig. 1(c). The error bounds on our ZTDSG exponent do not overlap with the percolation exponent range, nor with the first-order ϵ exponent for the $\frac{1}{2}$ state Potts model, nor with the series results of Ref. 17 for the thermal spin glass, $\gamma=2.9\pm 0.4$.

For $d=4$ and 5, the central ZTDSG values are higher than those of percolation. There is, however, some overlap in the error ranges. The exponents are clearly higher than the first-order ϵ expansion for the $q=\frac{1}{2}$ Potts but do not reach the series values for the thermal spin-glass exponents. Graphs of the analysis with $M2$ at $p=0.16475$ in $d=4$ and of the divided series with $M2$ in $d=5$ are given in Fig. 1(d) and 1(e), respectively.

In six dimensions, the logarithmic correction θ is close to, but above, that of percolation. It is not inconsistent with the value of $\frac{6}{17}$, which corresponds to θ for the $\frac{1}{2}$ state Potts model [$\theta=2(\partial_\gamma/\partial\epsilon)_{\epsilon=0}=\frac{6}{17}=0.353$]. In

higher dimensions, $\gamma=1.0$, as in all the problems discussed in this paper.

IV. CONCLUSIONS

In conclusion, we find that p_{SG} in the ZTDSG is always above the percolation threshold. This result is clear in every case.

As regards the exponent values, however, we cannot claim any decisive result. There is a general trend that in lower dimensions the exponent is not inconsistent with that of the thermal spin glass. At $d=4$ and $d=5$ we have a reasonably reliable comparison with the new thermal spin-glass estimates and can observe that the ZTDSG values fail to overlap with the thermal spin-glass values. On the other hand, the lower ends of the ZTDSG ranges are below the central percolation estimates. Thus we can only conclude that there is no evidence from the 15-term series that $\gamma(\text{ZTDSG})=\gamma(\text{SG})$ for general $d < 6$, although it may be observed in the lower dimensions.

All the numerical evidence is consistent with the scenario that there is a crossover from percolation to $q=\frac{1}{2}$ Potts to spin glass, and this crossover becomes more pronounced as the length of the series increases. It should occur for relatively shorter series in the lower dimensions, as we are sampling more loops there. The crossovers do not appear to be symmetric in the sense that the percolation to $q=\frac{1}{2}$ Potts crossover occurs relatively quickly as the series length is increased. Since the splitting between the different correlation functions⁴ (which causes the model to be in the same universality

class as the thermal spin glass) is very small in high dimensions, we expect that the $q = \frac{1}{2}$ Potts to spin-glass crossover will be very slow. In this case the value of γ (ZTDSG) that we have determined may not represent a true asymptotic value. The fact that our 3D value of γ (ZTDSG) does not coincide with that of Ref. 17 may be a consequence of this slow crossover and/or of the Ref. 17 value being a little too large. This matter will be discussed further in Ref. 16. It would be useful in the future to obtain better estimates for the $q = \frac{1}{2}$ state Potts model exponents in order to clarify these crossovers.

ACKNOWLEDGMENTS

This work was supported in part by grants from the Israel Academy of Sciences and Humanities, and by the U.S.–Israel Binational Science Foundation. Also, one of us (A.B.H.) acknowledges partial support from the Materials Research Laboratory (MRL) program of the National Science Foundation under Grant No. DMR 85-19059, and one of us (J.A.) acknowledges support from the Technion Vice President's Research Fund and the New York Metropolitan Research Fund.

-
- ¹A. Aharony, J. Phys. C **11**, L457 (1978).
²M. R. Giri and M. J. Stephen, J. Phys. C **11**, L541 (1978).
³A. Aharony and P. Pfeuty, J. Phys. C **12**, L125 (1979).
⁴A. B. Harris, J. Phys. A **20**, L1011 (1987).
⁵A. Aharony and K. Binder, J. Phys. C **13**, 4091 (1980).
⁶R. G. Palmer and F. T. Bantilan, J. Phys. C **28**, 171 (1985).
⁷B. Southern, A. P. Young, and P. Pfeuty, J. Phys. C **12**, 683 (1979).
⁸A. Benyoussef and N. Boccara, J. Phys. C **16**, 1901 (1983); Phys. Lett. **93A**, 351 (1983).
⁹A. J. Bray and S. Feng, Phys. Rev. B **36**, 8456 (1987).
¹⁰M. J. Stephen and G. S. Grest, Phys. Rev. Lett. **38**, 567 (1977).
¹¹O. F. de Alcantara Bonfim, J. E. Kirham, and A. J. McKane, J. Phys. A **13**, L247 (1980); **14**, 2391 (1981).
¹²J. Adler, A. Aharony, A. B. Harris, and Y. Meir (unpublished).
¹³R. M. Ziff and G. Stell (private communication).
¹⁴B. Nienhuis, J. Phys. A **15**, 199 (1982), and references therein.
¹⁵K. Binder and A. P. Young, Rev. Mod. Phys. **58**, 80 (1986).
¹⁶J. Adler, A. Aharony, A. B. Harris, L. Klein, and Y. Meir (unpublished).
¹⁷R. R. P. Singh and S. Chakravarty, Phys. Rev. B **36**, 559 (1987).
¹⁸R. Fisch and A. B. Harris, Phys. Rev. B **18**, 416 (1978).
¹⁹J. Adler, Y. Meir, A. B. Harris, A. Aharony, and J.A.M.S. Durat , Phys. Rev. B **38**, 4941 (1988).
²⁰A. B. Harris, Phys. Rev. B **26**, 337 (1982).
²¹A. B. Harris and Y. Meir, Phys. Rev. B **36**, 1840 (1987).
²²M. F. Sykes and M. K. Wilkinson, J. Phys. A **19**, 3425 (1986).
²³J. Adler, M. Moshe, and V. Privman, Phys. Rev. B **26**, 1411 (1982); J. Phys. A **14**, L363 (1981); J. Adler and I. G. Enting, *ibid.* **17**, 2233 (1984).
²⁴J. Adler and V. Privman, J. Phys. A **14**, L463 (1981).
²⁵Y. Meir, J. Phys. A **20**, L349 (1987).
²⁶D. S. Gaunt and H. Ruskin, J. Phys. A **11**, 1369 (1978).